doi:10.26443/seismica.v5i2.2561

SEISMICA

Improving seismicity monitoring to prepare for CO_2 storage in the Horda platform, Norwegian North Sea

Hasbi Ash Shiddiqi * [1,2], **Lars Ottemöller** [2], **Zoya Zarifi** [3], **Paul Martin Mai** [1]

[1]Physical Sciences and Engineering Division, King Abdullah University of Science and Technology, Thuwal, Saudi Arabia, [2]Department of Earth Science, University of Bergen, Bergen, Norway, [3]Equinor ASA, Stavanger, Norway

Author contributions: *Conceptualization*: HAS, LO, ZZ. *Methodology*: HAS, LO. *Software*: HAS, LO. *Validation*: HAS. *Formal Analysis*: HAS. *Investigation*: HAS. *Resources*: LO, PMM. *Writing - Original draft*: HAS. *Writing - Review & Editing*: HAS, LO, ZZ, PMM. *Visualization*: HAS. *Supervision*: LO, PMM. *Project administration*: LO, ZZ. *Funding acquisition*: LO, ZZ.

Abstract The Horda Platform in the Norwegian North Sea will host several awarded CO_2 storage licenses. This requires a robust understanding of background seismicity for site characterization and baseline monitoring. Offshore seismic monitoring is challenging when relying mainly on land stations, leading to poor azimuthal coverage and less precise locations. To improve monitoring in the Horda platform, we deployed three broadband ocean bottom seismometers (OBSs) during October 2021 to September 2022. We used ambient noise cross-correlations to validate OBS timing corrections, which also revealed Scholte waves consistent with the presence of soft sediments. We applied a deep learning-based detection algorithm to continuous OBSs and land data, followed by manual review. The resulting catalog, combined with the Norwegian National Seismic Network, reduced the magnitude of completeness to 0.8. Bayesian hierarchical relocation further refined event locations and increased confidence in detecting small earthquakes. The seismicity analysis revealed previously undetected offshore events, mainly north of the Horda Platform. These events are small and spatially scattered, but provide an improved baseline for seismicity characterization. Our work shows that long-term OBS deployment near the injection site enhances passive seismic monitoring plan for an offshore CO_2 storage site.

Production Editor:
Gareth Funning
Handling Editor:
Robert Skoumal
Copy & Layout Editor:
Mengjie Zheng

Signed reviewer(s):
J. Ole Kaven

Received:
January 30, 2026
Accepted:
June 25, 2026
Published:
July 14, 2026

Non-technical summary The Horda Platform in the North Sea is planned as a major site for underground CO_2 storage to support European Union (EU) climate goals. EU regulations recommend seismic monitoring to characterize storage sites and to establish a baseline before CO_2 injection begins. Such baseline data are important for identifying any changes in seismic activity that may occur after injection, for example due to pressure changes in the subsurface. At present, earthquake monitoring in this offshore area relies mainly on land-based instruments, which makes it difficult to detect and accurately locate small earthquakes beneath the seabed. To address this limitation, we deployed three seismometers on the seafloor for one year (2021–2022). These instruments significantly improved our ability to detect small earthquakes that would otherwise go unnoticed. We used machine learning to identify earthquake signals, followed by manual verification. These datasets also provided information about soft sediment layers that affect how seismic waves travel. The detected earthquakes were small and scattered, but they provide an important baseline for future CO_2 injection monitoring. This approach improves seismic monitoring for offshore CO_2 storage operations.

1 Introduction

The Norwegian North Sea is a region of low to moderate seismicity, with earthquakes mainly occurring within pre-existing structures along the Viking Graben and close to the coast of Western Norway (Figure 1). The stress regime is primarily controlled by the ridge-push forces from the Mid-Atlantic Ridge (Fejerskov and Lindholm, 2000). While large earthquakes are uncommon, historical events such as the 1927 M5.3 earthquake near the Viking Graben (Lee, 1932; Ringdal, 1983) indicate that stress slowly accumulates and is eventually released through fault reactivation (Bungum et al., 2003). Recently, two earthquakes have highlighted the potential for moderate seismic activity in the North Sea: the 30 June 2017 M_w 4.5 earthquake in the southern Viking Graben (Jerkins et al., 2020) and the 21 March 2022 M_w 5.1 event at the Tampen Spur near the Snorre oil field (Jerkins et al., 2023). Both of these had a thrust mechanism, consistent with the regional tectonics. The latter was widely felt across southern Norway and parts of Scotland, even prompting a short shutdown of a nearby offshore installation. These events show that despite the region's generally low seismicity, occasional moderate size earthquakes occur, which may cause concern for offshore industrial operations.

Current seismic monitoring in the Norwegian North Sea relies primarily on land-based stations from the Norwegian National Seismic Network (NNSN) and stations from neighboring countries (Figure 1). This setup results in higher location uncertainties for offshore

*Corresponding author: hasbi.shiddiqi@kaust.edu.sa

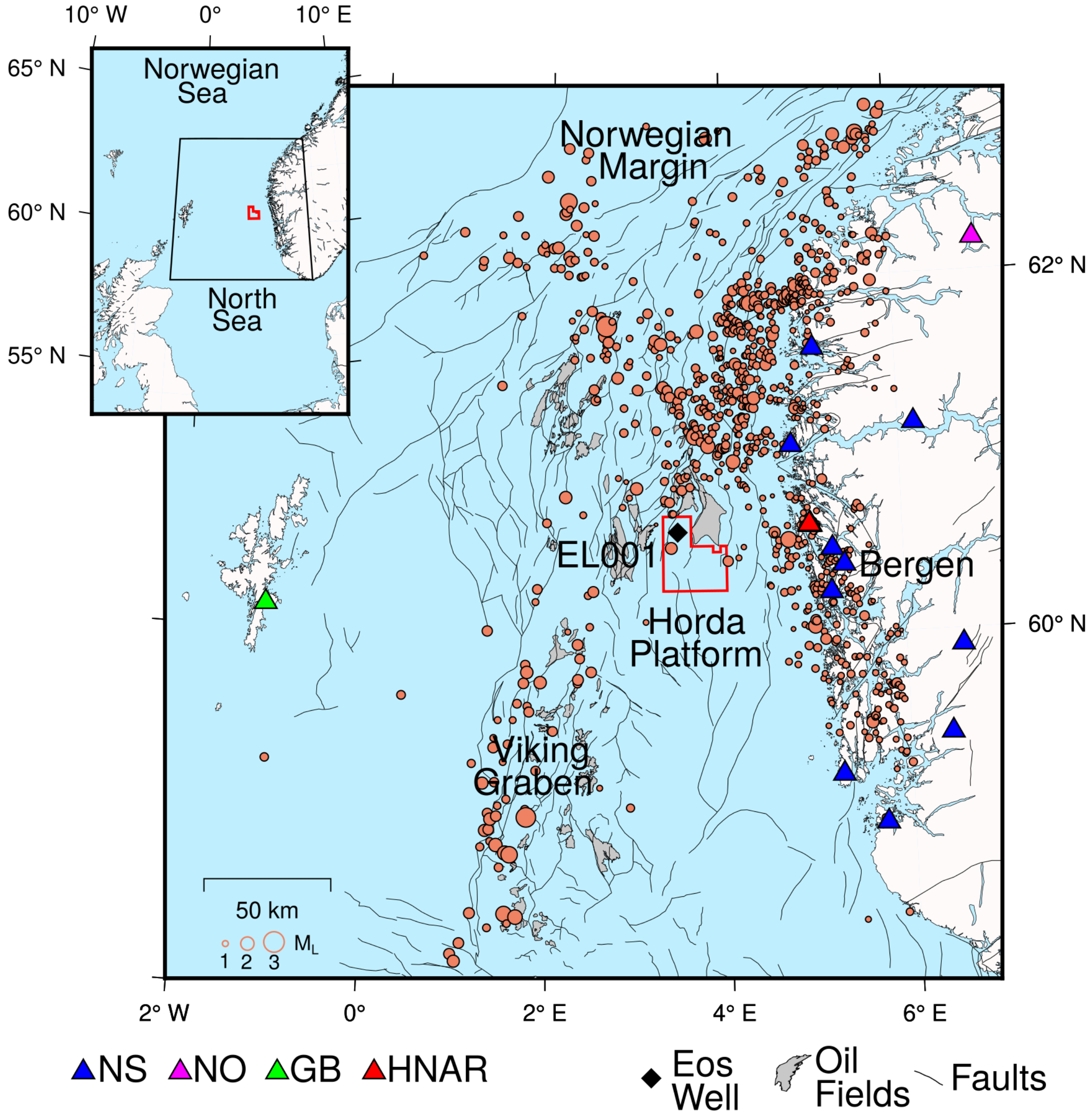

Figure 1 Seismicity and geological setting of the northern North Sea and nearby region. The earthquake catalog spans the year 2015 to 2022 and is provided by the Norwegian National Seismic Network. Seismic stations used to monitor the seismicity in the region are labeled as triangles. Fault and oil field database are provided by the Norwegian Offshore Directorate. Inset map in the top left shows the study area in larger geographical area.

events and limits earthquake detection capability. Recent enhanced monitoring onshore southwestern Norway using temporary seismic deployments has demonstrated improved detection capabilities and reduced magnitude of completeness (Marck et al., 2025). The NNSN has access to offshore geophone sensors that are part of permanent reservoir monitoring systems from some oil fields. However, these networks are spatially constrained and affected by high ambient noise levels from production activities. To more reliably observe small induced events, there is an urgent need for better offshore monitoring to improve both detection and location accuracy.

This monitoring challenge becomes more important as Norway expands its carbon capture and storage activities, which may lead to a localized increase in seismicity alongside the region's natural earthquakes. The Aurora CO_2 storage project (License EL001) is part of Norway's larger carbon capture and storage initiative to securely store CO_2 in deep saline aquifers within the Horda Platform, a structural high located between the Viking and Sogn grabens about 90 km west of Bergen (Furre et al., 2019) (Figure 1). The Johansen Formation, located at approximately 2,500–3,000 meters depth, has been identified as a suitable reservoir, with porous sandstone for CO_2 storage and a thick caprock layer providing necessary containment (Eigestad et al., 2009). The suitability of this reservoir was further evaluated through the drilling of the Eos injector well (e.g., Holden et al., 2022; Thompson et al., 2022) (see Figure 1 for the well location). However, fluid injection alters subsurface stress conditions, which can lead to

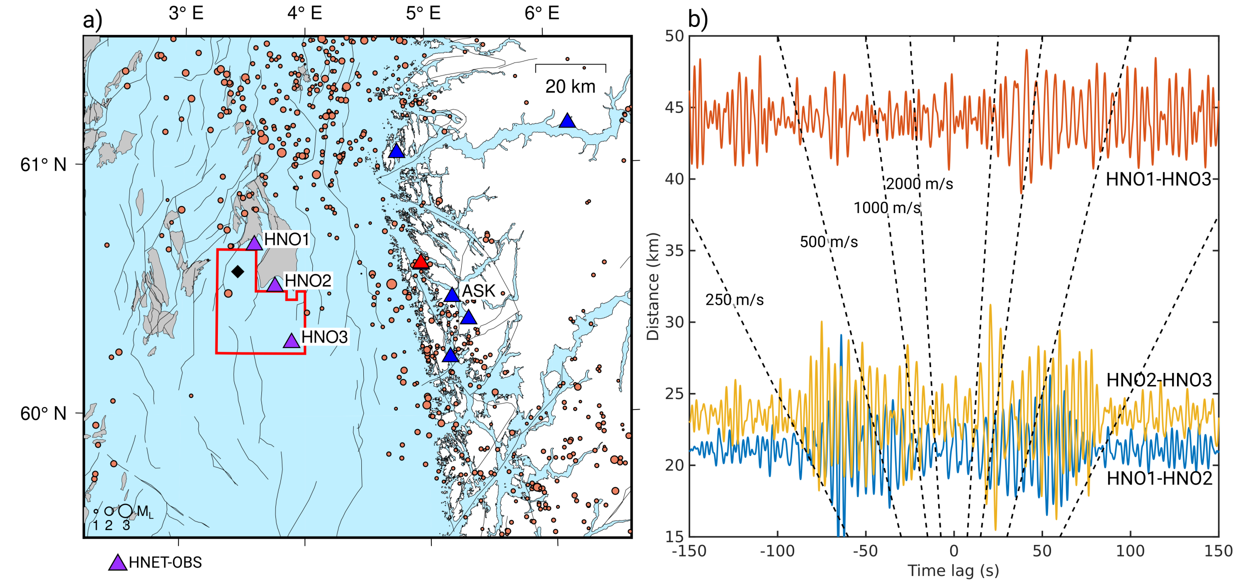

Figure 2 a) Seismicity map around the the EL001 site and the location of three OBSs deployed during HNET project. b) Empirical Green's Functions derived using cross-correlation between OBS pairs. Dashed lines show the group velocity in the range of 250 m/s to 2000 m/s.

induced seismicity (Zoback and Gorelick, 2012). Previous studies have shown that even minor pressure changes from CO_2 injection may trigger microseismicity, emphasizing the need for continuous monitoring (e.g., Goertz-Allmann et al., 2014; Kaven et al., 2015). It is worth noting that other types of fluid injection have induced larger-magnitude earthquakes in some regions (Ellsworth, 2013; Grigoli et al., 2018; Ge and Saar, 2022). For instance, observations from the In Salah CO_2 storage project in Algeria have demonstrated that fluid injection reactivates pre-existing fractures, leading to detectable seismic activity (Goertz-Allmann et al., 2014). Similarly, at the Decatur CO_2 sequestration site in Illinois, USA, surface monitoring has revealed how subtle pressure perturbations generate seismicity within the reservoir (Kaven et al., 2015). Pressure changes associated with CO_2 injection may induce microseismicity by promoting slip on pre-existing faults and fractures (e.g., Zoback and Gorelick, 2012; Goertz-Allmann et al., 2014; Kaven et al., 2015). Therefore, good baseline seismic monitoring is needed for both safety and regulatory requirements.

To improve seismic monitoring in the Horda Platform, the Horda Seismic Network (HNET) project was installed to enhance earthquake detection and location accuracy in northern North Sea using a seismic array and OBSs (Zarifi et al., 2022) (Figure 1). In October 2021, three broadband OBS units were deployed and remained operational for a year. In this study, we investigate how integrating the OBSs with land-based stations help improve the earthquake monitoring capabilities in the Norwegian North Sea, particularly around the Horda platform. We analyze earthquake catalogs and waveforms to measure changes in detection ability and location accuracy. The findings reveal how offshore-onshore networks assist in better monitoring both background seismicity and potential injection-induced events in CO_2 storage areas.

2 OBS deployment and data pre-processing

To improve seismic monitoring around the Aurora field, the University of Bergen and Equinor deployed three broadband Nammu OBSs manufactured by K.U.M. (Umwelt- und Meerestechnik Kiel GmbH) (Figure 2). Each OBS, equipped with a three-component Nanometrics Trillium compact seismometer and a hydrophone, was deployed in shallow waters (280–316 meters depth) from October 2021 to September 2022. The OBSs (HNO1, HNO2, and HNO3) were deployed on the western edge of the Aurora license area to obtain good regional coverage, with HNO1 located 14 km from the Eos CO_2 injector well (Figure 2). An important criterion in the selection of deployment locations was to avoid areas that are affected by fish trawling.

The internal clocks of the OBSs were synchronized with GPS time before and after deployment, and skew measurements were taken (Table 1). However, previous studies have reported nonlinear clock drift in some OBS deployments (Loviknes et al., 2020; Pilot et al., 2024) and it is important to verify the timing. Following Loviknes et al. (2020) and Naranjo et al. (2024), we used ambient noise cross-correlation to independently verify the OBS clock skew measurements, using the EGF_td_toolbox (Loviknes, 2018). Following Bensen et al. (2007), before performing cross-correlation, we preprocessed the data by removing the mean and trend, applying a taper, and correcting for instrument response. Example of empirical Green's functions (EGFs) between OBS pairs are shown in Figure 2.b. Cross-correlation between station pairs (HNO1-HNO2, HNO2-HNO3, HNO1-HNO3) was used to assess time shifts and verify skew corrections. Details of the data processing for time correction are presented in the supplementary material (Text S1). Figure 3 shows an example of relative time delay measurement between HNO2 and HNO3. Ambi-

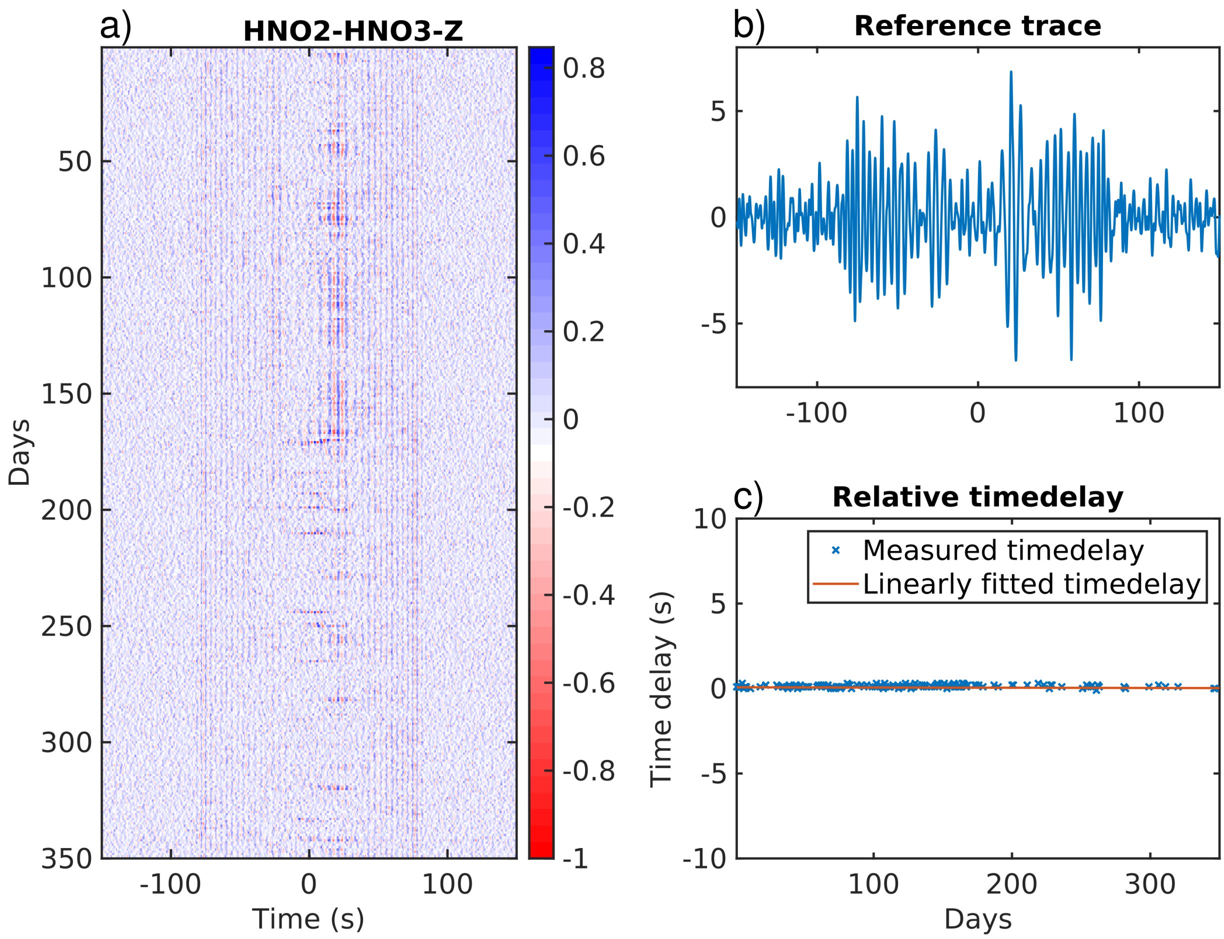

Figure 3 a) Daily empirical Green's function extracted from ambient noise correlation of skew corrected OBSs: HNO2 and HNO3. b) Reference trace, filtered between 0.1 and 0.5 Hz, used to measure time delay. c) Relative time delay between OBSs HNO2 and HNO3, which show no relative time drift between these skew corrected traces.

ent noise cross-correlation shows that the time drifts are linear and match with the skew measurement (Table 1). Therefore, we decided to use the skew measurement to correct for the continuous seismic data.

When OBSs are deployed using free-fall methods, the horizontal channel orientation becomes unknown (labeled as HHY and HHX). To obtain the correct orientation, we first tried using surface waves from distant earthquakes and body waves from regional earthquakes (e.g., Doran and Laske, 2017; Parisi et al., 2024), but the signal quality was too low. Instead, we used seismic air-gun shots from the Smeaheia license area (20-40 km from the OBSs), with precise source location and timing provided by Equinor (Figure 4.a). We analyzed the early part of these signals and calculated the apparent back-azimuth using polarization analysis of the horizontal channels (Figures 4.b and Figure 4.c).

The orientation process works as follows: if the horizontal channels are correctly aligned with north-south and east-west directions, the back-azimuth measured from polarization should generally match the actual back-azimuth between the receiver and source (with a 180° ambiguity). We rotated the channels (HHY and HHX) clockwise by an angle (α) calculated from the difference between measured and actual back-azimuths. To resolve the 180° ambiguity, we then used two approaches: comparing polarities between horizontal and vertical channels, and checking that radial and vertical channel polarities match expectations (Havskov and Ottemöller, 2010). When polarities of the radial and vertical channels differed, we adjusted the rotation angle by 180°. Details of the data processing for horizontal channel orientation determination are summarized in the Supplementary material (Text S2). The final orientation of horizontal channels are shown in Table 2.

Background seismic noise levels affect seismic monitoring capability. To evaluate the noise, we computed the power spectral density (PSD) of the three OBS components and compared these with a nearby land-based permanent station ASK that is installed on bedrock. We computed the noise PSD following the methods of McNamara and Buland (2004) (Figure 5). As expected, the OBS stations exhibited higher noise levels than the ASK station on the western coast near Bergen, with differences of up to approximately 20 dB at 10 Hz, particularly on the horizontal channels. The seismic noise levels exhibit seasonal variations that differ across frequency bands. At longer periods ($>$ 5 seconds), noise levels are consistently higher in winter than summer for both OBS stations and the ASK station, likely reflecting increased storm activity and ocean wave heights during winter months (Figure S1 in the supplementary material). Conversely, at shorter periods ($<$ 0.5 seconds), noise levels are higher in summer than winter,

Table 1 Time correction for OBSs obtained from skew measurement and ambient noise cross-correlation

Station	Skew (seconds)	7-day stack (seconds)	daily EGF (seconds)
HNO1	-29.446	-28.9	-29.4
HNO2	-3.0199	-3.0	-3.0
HNO3	-0.4220	-0.4	-0.4

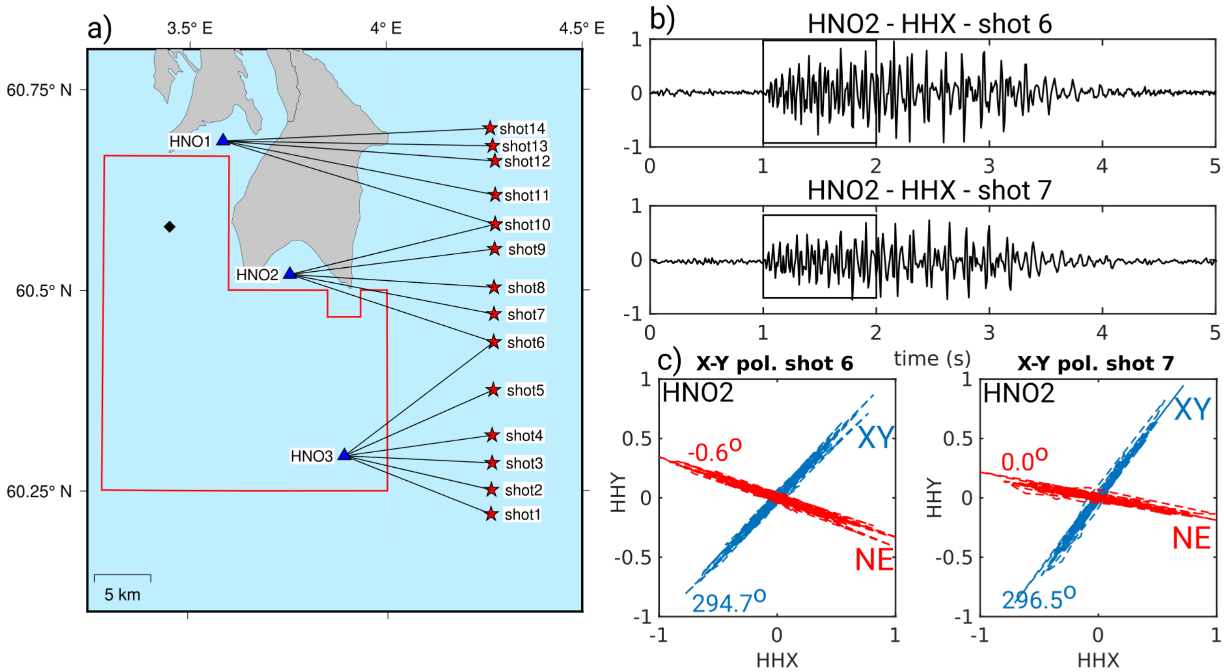

Figure 4 a) Distribution of 14 seismic shots used to determine orientation of horizontal channels. The black lines represent the path from the sources to OBSs. b) Example of two seismic shots, shot6 and shot7, recorded by HNO2 on HHX channel. The black rectangles show the one second time window used for signals used for polarisation analysis. c) Polarisation analysis for horizontal channels of HNO2: HHX-HHY (blue lines) and rotated channels HHE-HHN (red lines). The difference between back azimuth measured with geographical coordinate and polarisation analysis for HHX-HHY and HHE-HHN channels are shown in blue and red text, respectively.

with this pattern being more pronounced at the OBS stations than at ASK. This frequency-dependent seasonal variation suggests different noise sources dominating at different periods, with long-period noise controlled by ocean-meteorological conditions and short-period noise potentially influenced by increased summer anthropogenic activity.

Most stations in Norway generally exhibit low noise levels relative to the noise models of Peterson (1993) as reported by Demuth et al. (2016). The observed level of ca. -120 dB at 0.2 s, as on the OBSs, would be acceptable levels even on land in more noisy locations. Amplification due to sedimentary layers may contribute to the higher noise level (Corela et al., 2023; Dewangan et al., 2017; Parisi et al., 2024). The high-frequency noise (periods below 1 second) is notably higher at the OBSs, likely due to nearby anthropogenic activities and thick sedimentary layers ($>$ 5 km) (Fazlikhani et al., 2017). In comparison, the same OBSs deployed in the Arctic region (Svalbard) showed lower noise levels at similar frequencies (Jeddi et al., 2021), where sedimentary layers are thinner (1-2 km) (Funck et al., 2017).

3 Observation of Scholte Wave

Cross-correlation functions serve both as a tool for validating OBS timing and as a means of characterizing the seismic wavefield. The EGFs obtained in this study (Figure 2.b) exhibit a more complex waveform structure than EGFs reported from OBS deployments in other regions, such as western Svalbard (Jeddi et al., 2021), the western Indian Ocean (Hable et al., 2018), and the Cascadia subduction zone (Rathnayaka and Gao, 2017). In particular, the waveforms show extended, high-amplitude arrivals that are not typically observed in deeper-water or less sedimented environments, suggesting that local offshore conditions play a significant role in shaping the recorded signals. Understanding the shallow offshore structure is important because low-velocity sediments and the water column strongly affect ambient noise wavefields and surface waves recorded by OBS stations. These effects can influence waveform characteristics and offshore earthquake monitoring.

Inspection of the EGFs reveals two distinct phases with different propagation characteristics (Figure 2.b). The earlier arrivals have relatively low amplitudes and exhibit group velocities ranging from approximately 500 m/s to 2000 m/s. In contrast, the later arrivals

Table 2 Azimuth of horizontal channels measured clockwise from north and the clockwise rotation angles for the OBSs

OBS	HHY azimuth	HHX azimuth	Rotation Angle	Uncertainty
HNO1	140.8°	230.8°	219.2°	± 2.2°
HNO2	244.0°	334.0°	116°	± 1.4°
HNO3	234.4°	324.4°	125.6°	± 1.8°

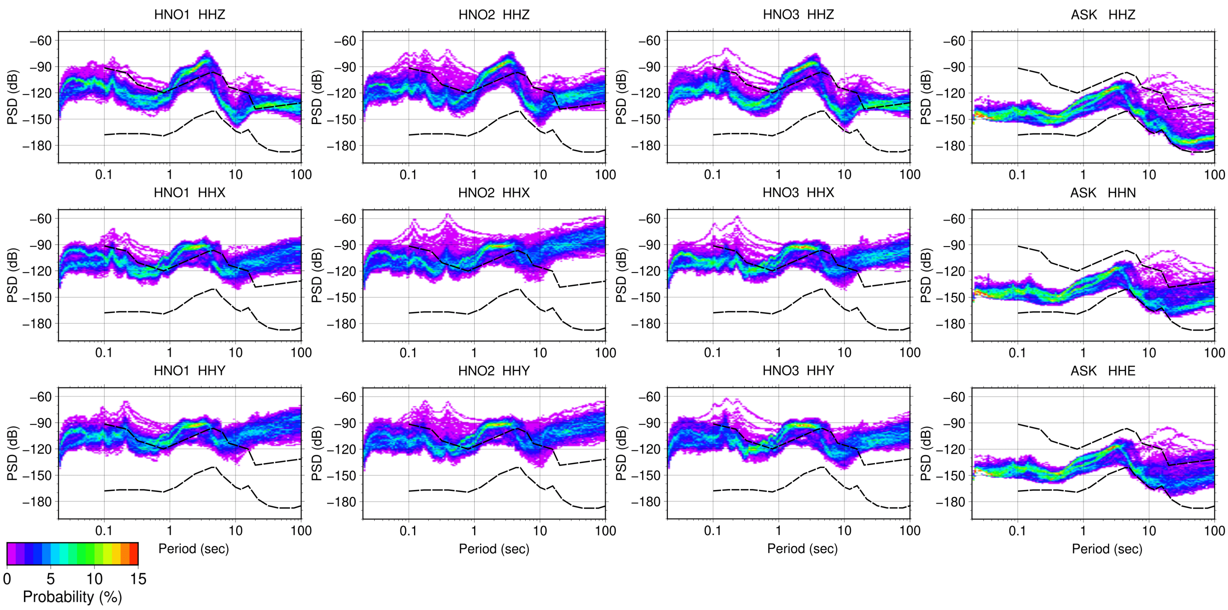

Figure 5 Probabilistic power spectral density (PPSD) of seismic noise for all OBSs and one permanent seismic station (ASK) located in the west coast of Norway. The PPSD plots of the OBSs show elevated noise level in all frequency bands.

display higher amplitudes and lower group velocities, ranging from 250 m/s to 500 m/s. This combination of low velocity, high amplitude, and prolonged wave trains is characteristic of Scholte waves, which propagate along the interface between the water column and the seafloor (Delaney et al., 2017). The prominence of this wave train in our EGFs indicates that interface-guided waves dominate the ambient noise correlations in this shallow, sediment-rich offshore setting. Characterizing these interface-guided waves helps explain the observed ambient noise correlations and the influence of shallow sediments on offshore seismic monitoring.

To investigate the origin of the observed waveforms, we examined the effects of the water column and shallow sedimentary structure on surface wave propagation using forward modeling. Synthetic surface waves were generated with the Computer Programs in Seismology package (Herrmann, 2013). As a reference, we adopted a 1-D V_P model derived from the nearby Snorre field provided by Equinor and systematically modified its upper layers. We tested a range of scenarios by varying the properties of the shallow section, including a water layer, the addition of low-velocity sedimentary layers beneath the seafloor, V_P reductions of 0% to 25% relative to the reference model, and V_P/V_S ratios between 1.74 and 3.0. Following Nguyen et al. (2009), the seismic source was placed at the ocean bottom and modeled as an explosive mechanism to efficiently excite surface waves.

Representative velocity models and corresponding synthetic waveforms are shown in Figure 6. The reference Snorre-based model (model sea 1) could not reproduce the observed EGF waveforms, even when using a V_P/V_S ratio of 1.8. Introducing a single low-velocity sedimentary layer with an elevated V_P/V_S ratio of 2.5 (model sea 2) produces delayed arrivals but does not reproduce the extended, low-velocity wave trains observed in the data. A closer match to the observed EGFs occurs only when an additional low-velocity layer is included beneath the water column, V_P 1500 m/s, V_S 500 m/s and V_P/V_S ratio of of 3.0 is assigned to this layer (model sea 3). Geologically, this low-velocity layer likely represents water-saturated, poorly consolidated near-seafloor sediments, rather than consolidated sedimentary rocks (e.g., Nguyen et al., 2009; Kugler et al., 2007). These results indicate that both the presence of the water column and thick, soft sediments are required to explain the dominant low-velocity phases in the EGFs.

In summary, the observed group velocities, waveform characteristics, and modeling results consistently indicate that Scholte waves are a major contributor to the ambient noise EGFs recorded by the OBS network. These observations show the strong influence of shallow offshore structure on seismic wave propagation in the study area.

4 Earthquake Data Processing

To evaluate the contribution of OBSs to earthquake monitoring, we added OBSs waveforms to the existing

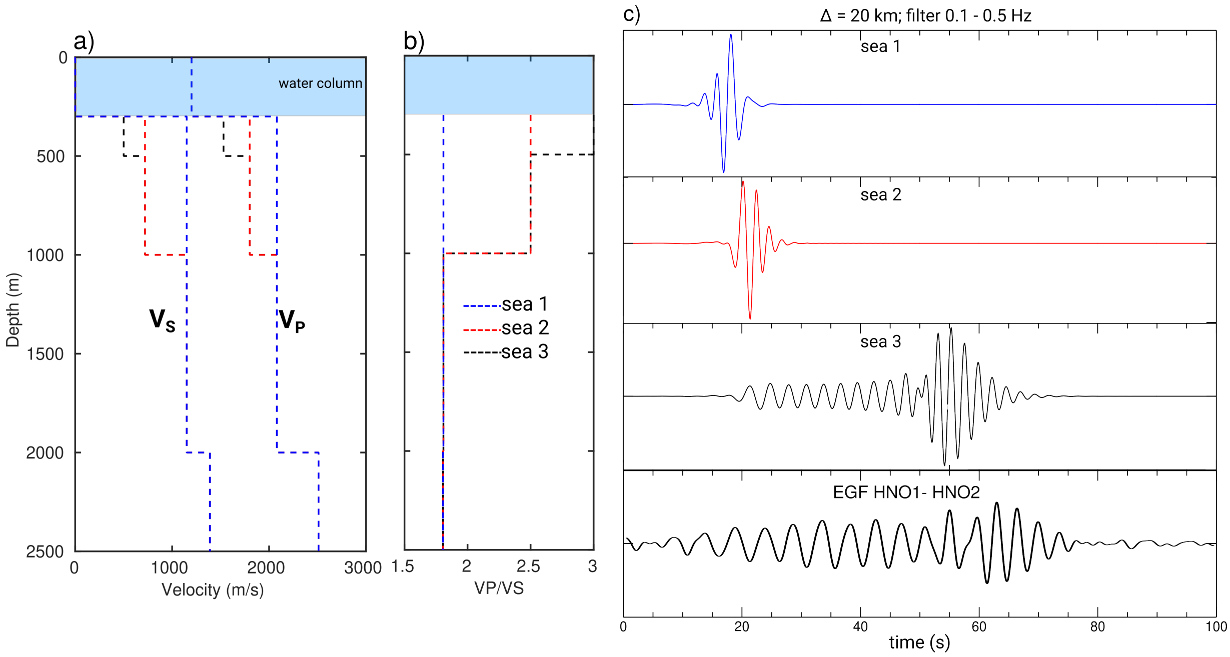

Figure 6 Surface wave modeling with models that include water column at the top (models sea 1, 2 and 3). The seismic source is placed at the bottom of the water column (300 m depth). The 1-D V_P and V_S models are shown in a) and the V_P/V_S ratios are shown in b). c) Synthetic vertical channel traces located at 20 km away from the source (sea 1, 2 and 3) and EGF for the station pair of HNO1 and HNO2 (EGF HNO1-HNO2). The traces are bandpass filtered between 0.1 to 0.5 Hz.

NNSN data from October 2021 to September 2022. We started by manually picking the P- and S-arrivals of the events recorded on the OBSs using the SEISAN software package (Havskov and Ottemoller, 1999; Havskov et al., 2020). This initial analysis of 76 earthquakes gave us 97 P-phases and 92 S-phases from the OBSs. While this manual approach provided reliable picks, we wanted to expand our detection capabilities.

To expand the catalog, we applied the deep-learning algorithm, EQTransformer (EQT) (Mousavi et al., 2020) to the continuous datasets. We used data from the OBSs together with land-based stations located in western Norway: University of Bergen Seismic Network (code NS), NORSAR (NO) and HNAR array (QE), and one station from the Great Britain Seismograph Network (GB) in Shetland island to increase the coverage. The EQT algorithm was trained using the STanford EArthquake Dataset (STEAD) (Mousavi et al., 2019). Previous studies have shown that this algorithm had been used in Northern and Southern Norway and had successfully lowered the detection threshold (Shiddiqi et al., 2023a,b; Marck et al., 2025). Comparison between EQT and manual picks for both OBSs and land stations showed differences generally within 0.15 s. Based on this good agreement, we manually checked and corrected picks when needed using the SEISAN package. Figure 7 shows the epicenter of an M_L 2.3 event and the vertical traces along with the P-picks.

Once we had reliable arrival times, we located the events using the Hypocenter program (Lienert and Havskov, 1995). The travel-time table was generated using the NNSN 1-D velocity model (Havskov and Bungum, 1987). However, not all detected events were natural earthquakes. For events near the coast, we classified events as explosions or blasts when their locations were close to known quarries or major construction sites. To confirm these identifications, we verified them using spectral analysis by looking for spectral banding (Ottemöller et al., 2018). After removing these non-natural events, the combined EQTransformer analysis using both OBS and land stations resulted in 154 additional events. For comparison, applying EQTransformer using only land stations resulted in 137 additional events. The relatively modest increase associated with the OBS data likely reflects the higher noise levels at the OBS sites and the concentration of much of the seismicity closer to the coast, where land stations already provide good detection capability.

The final step involved determining earthquake magnitudes. To determine earthquake size, we computed local magnitude M_L for the events. Following the procedure at the NNSN, we measured the maximum amplitude from the vertical traces of simulated Wood-Anderson seismograms and applied the M_L scale developed for Norway (Alsaker et al., 1991). The M_L for additionally detected events range between -0.3 and 1.7. Combining our results with existing data, we merged the newly detected events with the NNSN catalog and used the merged catalog for analysis for the time period of October 2021 to September 2022 (Figure 8). This integrated dataset reduced the estimated magnitude of completeness (Mc), estimated using Wiemer and Wyss (2000), dropped from Mc 1.1 to Mc 0.8 (Figure 8.b). Figure 9 shows the earthquake location parameter changes for datasets using only land stations and the combination of land stations and OBSs. The combined workflow improved the detection of low-magnitude seismicity, improving our understanding of local seismicity patterns.

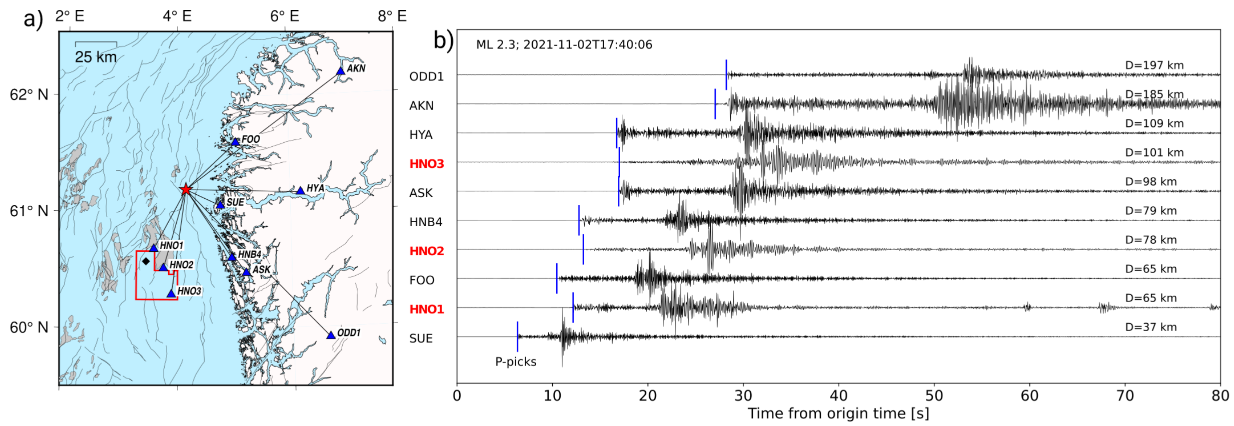

Figure 7 a) Example of an offshore earthquake, with M_L 2.3 and the travel-path to the seismic stations within hypocentral distance of 200 km. b) Vertical traces from the seismic stations within 200 km, filtered between 2-20Hz. P-picks are shown as blue vertical bars. Notice that the P-arrivals for OBSs, HNO1, HNO2 and HNO3, are slightly later than other stations with similar hypocentral distances.

5 Bayesian Hierarchical Earthquake Location

To better understand the earthquake locations and their uncertainty using the OBSs, we applied the Bayesian seismic event location algorithm (Bayesloc) (Myers et al., 2007, 2009). The Bayesloc algorithm formulates the joint probability distribution of multiple-event location parameters, such as event hypocenters, travel-time corrections, pick uncertainties, and phase labels. It uses Markov Chain Monte Carlo (MCMC) sampling to explore the joint probability distribution of these parameters. Subsequently, we analyzed the results to estimate the most likely hypocenters for the events. A key advantage of Bayesloc is that it accounts for the effect of velocity variations, in our case between offshore and onshore regions, by exploring the travel-time corrections on the input 1-D velocity model.

We designed our analysis to directly test the benefit of adding OBSs data. We relocated 159 events that were recorded by both land stations and OBSs. To compare the effect of OBS data, we ran two sets of inversions: using only land stations and using a combination of OBSs and land stations. We applied 10,000 MCMC iterations across 10 chains in Bayesloc, with a burn-in period of 1,000 iterations. The phase pick uncertainty was modeled using Gamma distribution as a prior, with shape parameter 0.05 and rate parameter 0.05, corresponding to a broad distribution centered around a standard deviation of approximately one second. We also needed to account for systematic biases in our travel-time predictions. Systematic travel-time residuals were accounted for by estimating station-specific and station-phase-specific corrections, allowing for flexible correction of unmodeled path effects and sensor timing biases. We did not fix the phase labels to correct possible mislabeling between direct Pg, Sg phases and Moho refracted phases Pn, Sn. Travel times were calculated using the NNSN 1-D velocity model, which does not capture all the complexity of the region (e.g., Fazlikhani et al., 2017; Crowder et al., 2021). The Bayesloc algorithm accounts for lateral heterogeneity between the offshore North Sea and the onshore crust of western Norway through empirical travel-time corrections.

Before looking at the location results, we examined how the algorithm characterized the different station types. We compared two sets of station-specific parameters estimated by Bayesloc: the arrival-time-error station precision factors (κ_j) and the travel-time correction terms (ϕ^{st}), to evaluate differences between OBSs and land-based stations (Figure S10 in the supplementary material). The results showed clear differences between the two station types. The three OBS stations (HNO1-HNO3) had lower mean κ_j values (mean = 0.47, mean SD = 0.23) than the land stations (mean = 1.02, mean SD = 0.40), indicating higher uncertainty in arrival times at OBS sites, probably due to higher noise levels. The travel-time corrections also showed interesting patterns. For the travel-time correction terms ϕ^{st}, the OBS stations showed higher mean station shifts (mean = 0.42 second, mean SD = 0.18 second) compared to the land stations (mean = 0.01 second, mean SD = 0.20 second). These higher correction factors at OBS sites likely reflect path effects or local structural heterogeneity not captured by the 1-D velocity model, particularly due to thick sedimentary layers offshore.

With this understanding of the station characteristics, we further examine the location improvements. The results from Bayesloc show the improvement in location accuracy when both OBSs and land stations are used. For the 159 events, the combination of OBSs and land stations reduced the average location standard deviation by about 30% in the horizontal direction and 26% in depth, compared to using land stations alone (Figure S11 in the supplementary material). This improvement can be attributed to the better spatial distribution of monitoring stations for offshore seismic activity. We can see this effect clearly in specific examples. Additional detail is shown in Figure 10, which presents the sampled locations from all iterations for four selected offshore events near the Horda platform. We computed the location uncertainty in the horizontal (XY) direction, illustrated by the 99% confidence error ellipsoids. When OBSs are included, the ellipsoids become smaller, showing that the posterior distribution of the event locations is more focused. These results demonstrate that integrating OBS data improves offshore earthquake locations.

6 Discussion

We deployed three broadband OBSs near the Aurora CO_2 storage site from October 2021 to September 2022, marking the first such offshore seismic monitoring study for this region in the Norwegian North Sea. The data reveal important characteristics of the subsurface structure and regional earthquake activity that inform monitoring strategies for planned CO_2 injection operations.

6.1 Enhancing regional seismic monitoring with OBS

Reducing the detection threshold at CO_2 storage sites is important as induced earthquakes are usually small (M < 2.0) and often missed by networks with few stations. Using deep-learning automated processing with manual checks lowered our magnitude of completeness from Mc 1.1 to Mc 0.8. We identified several offshore events north of the Horda Platform that were absent from the NNSN catalog, suggesting higher background activity than previously recognized.

During our monitoring period, no earthquake occurred directly in the Aurora license area. However, the wider region does have some diffuse seismic activity. This scattered pattern is normal for continental stable regions, where earthquakes occur along old weak zones rather than active fault lines (e.g., Marck et al., 2025). Event locations cluster along the western Norwegian coast and in offshore areas north of the Horda platform. This distribution matches the general locations of larger historical earthquakes, including the 1927 M 5.3 Viking Graben event (Lee, 1932; Ringdal, 1983) and the recent 2017 and 2022 earthquakes. Most events occurred at depths of 5-15 km, typical for the North Sea region. Only two events exceeded magnitude 2.0 during our monitoring period, confirming the generally low seismicity of the area but also showing that moderate events can still occur.

The Bayesian hierarchical relocation addresses velocity model uncertainties by explicitly modeling traveltime differences between offshore and onshore regions, providing improved relative locations critical for distinguishing induced from natural seismicity. These advances demonstrate the value of OBS networks for improving offshore seismic monitoring.

Poor azimuthal coverage is a fundamental limitation of land-based monitoring in offshore regions. This geometric constraint has been a persistent challenge in marine seismology, as demonstrated by studies in the Arctic (Jeddi et al., 2021) and the Red Sea (Shiddiqi et al., 2025), where onshore networks produce large location uncertainties for offshore events. Our results confirm that even a three-station OBSs array combined with the land network can improve the ability to detect and locate earthquakes offshore through better station coverage.

Knowledge of the seismic noise is important when estimating detection levels for seismic networks. As OBS experiments are normally done in deeper waters, little was known about noise levels in the coastal areas of the North Sea. Our OBS measurements confirmed expectations that the shallow ocean floor exhibits higher noise levels across all frequencies than coastal stations on land, especially on the horizontal channels. Thick sediments under our sites (over 5 km) are likely to amplify noise as other studies have found (Corela et al., 2023). The noise characteristics have important implications for detection thresholds and monitoring strategies. Unlike land stations with optimal performance across broad frequency ranges, OBSs performance varies significantly with local conditions, including sediment thickness, ocean currents, and anthropogenic activities. For CO_2 storage monitoring, where small-magnitude events are critical, understanding these noise limitations becomes essential for network design.

Scholte waves recorded across the OBS network exhibit group velocities between 250-500 m/s, indicating substantial sedimentary layers beneath the seafloor. Our surface wave modeling demonstrates that V_P/V_S ratios of approximately 3.0 are required to reproduce the observed dispersion, indicating poorly consolidated marine sediments in which shear-wave velocities are strongly reduced (e.g., Nguyen et al., 2009). This consistency between our seismic observations and existing geological knowledge supports our interpretation. The observed EGF patterns are comparable to observations from other continental margins like Cascadia (Rathnayaka and Gao, 2017) and Ninetyeast Ridge (Nguyen et al., 2009), and studies in the North Sea with smaller interstation distances (e.g., Bussat and Kugler, 2011).

Our surface wave modeling shows that the water column and soft sedimentary layers influence surface wave propagation between the OBS. The group velocity of the later part of the surface wave falls within the range of Scholte waves, which travel along the boundary between the water column and the seafloor. Identifying these waves helps explain the complex character of our EGFs and the distinct seismic behavior in the offshore North Sea environment. The sediment layers also affect wave propagation and the accuracy of locating small earthquakes that may accompany injection operations. Understanding these effects is essential for developing reliable monitoring strategies, and accurate 3-D velocity models that include shallow structural variations will be needed for precise earthquake locations during injection activities.

6.2 Monitoring Strategy for CO_2 Storage Operations

Our results support a monitoring approach that combines OBSs with existing land-based networks. Land stations have lower noise conditions providing better detection, while OBS can be placed closer to sources offshore and improve network geometry. Careful place-

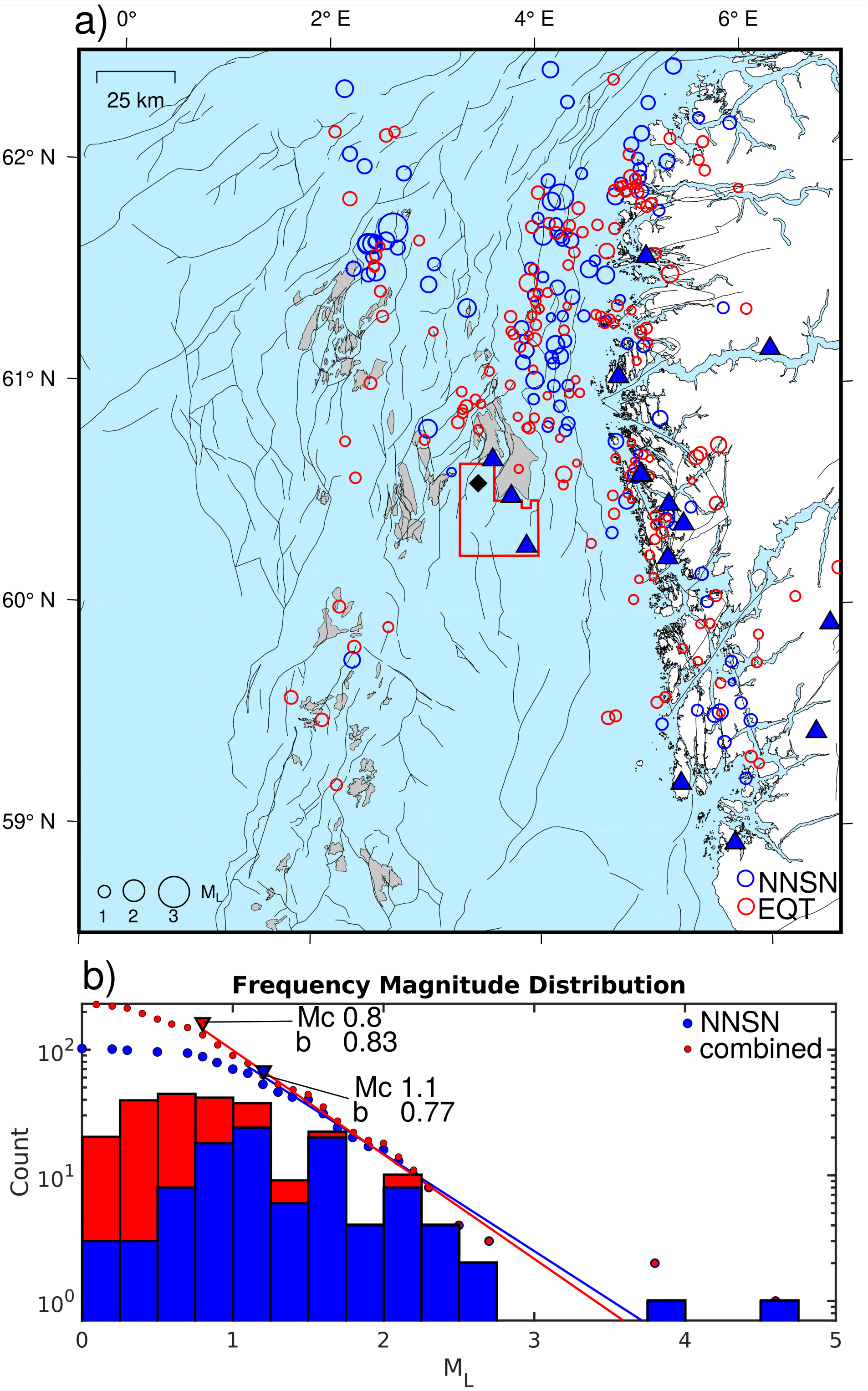

Figure 8 a). Seismicity map showing the events reported by the NNSN and new events detected using EQT, showed as blue and red open circles, respectively. b) Frequency magnitude distribution between NNSN and combine NNSN and EQT catalogs. The combination of NNSN and EQT catalogs suggests reduction of magnitude of completeness (Mc) from 1.1 to 0.8

ment of permanent OBS units near injection sites would optimize monitoring coverage. Implementation of automated processing with real-time data transmission could detect injection-induced seismicity within minutes, allowing rapid response to unusual activity (e.g., Bussat et al., 2016, 2018; Schultz et al., 2023). Real-time microseismic monitoring has proven valuable at several CO_2 storage sites for detecting changes in seismic activity patterns during injection operations (e.g., Verliac and Calvez, 2021; Chen et al., 2022; Shen et al., 2022). Our results with three temporary OBS demonstrate that a permanent network of strategically placed small number of OBSs could provide an improved coverage for the Aurora storage area. Integration with existing reservoir monitoring systems at North Sea oil fields could provide complementary information about both earthquake ac-

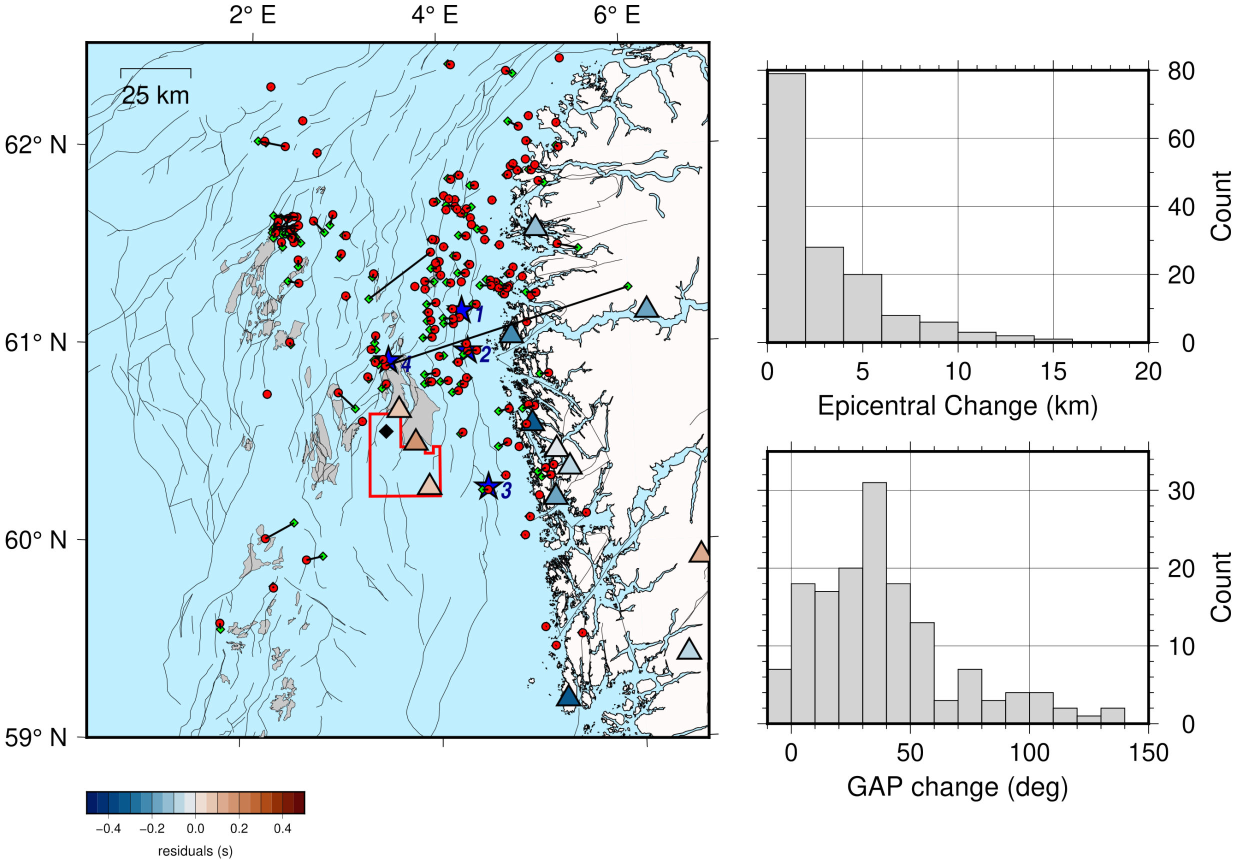

Figure 9 Variations in earthquake locations between land stations only and combination of land stations and OBSs. a) Map showing epicentral shifts. Blue stars labelled with event numbers show the locations of selected earthquakes shown in Figure 10. b) and c) shows the histograms showing the epicentral and azimuthal gap changes, respectively

tivity and reservoir behavior.

Beyond traditional seismic monitoring, emerging technologies, such as distributed acoustic sensing (DAS), offer complementary surveillance capabilities. DAS systems have shown particular promise for CO_2 storage monitoring in both Arctic and North Sea environments. Recent work demonstrates the potential for existing telecommunications infrastructure. Landrø et al. (2022) used DAS on a fiber-optic cable from Svalbard to mid-Norway to detect whales, storms, ships, and earthquakes. Similarly, Baird et al. (2025) demonstrated ocean surveillance capabilities using DAS on North Sea submarine telecommunications cables, including ability to detect and locate underwater explosions, local earthquakes, and atmospheric events. Their real-time processing workflow distinguished between seismic body waves, hydroacoustic waves, and infrasound, showing that existing North Sea cable networks could support comprehensive monitoring operations.

While DAS can capture seismic signals comparable to conventional instruments when deployed near the source region, recent studies indicate that its signal quality is more spatially variable and sensitive to environmental conditions, cable coupling, and source–receiver geometry (e.g., Frazão, Orlando et al., 2026; Cubas Armas et al., 2026). For example, comparison with OBSs show that DAS observations can provide useful seismic information but typically require calibration, filtering, and selection of high-quality channels due to variable noise conditions. In contrast, OBS recordings provide more stable point measurements of ground motion, making the two approaches complementary for offshore monitoring.

Our temporary OBS deployment provides practical experience for improving passive seismic monitoring in offshore CO_2 storage sites. While its limited duration prevents assessment of long-term background changes, the results demonstrate that short-term OBS deployments may enhance detection and location accuracy in offshore settings. Integrating seismic monitoring with structural and geological information through 3-D imaging and potential field data will help clarify the relation between faults and observed seismicity. The methods and observations presented here form a useful basis for future monitoring at sites such as the Aurora project. Combining improved background characterization, refined detection capabilities, and improved velocity models support safe and efficient CO_2 storage operations in similar offshore environments.

7 Conclusions

This study demonstrates that a small offshore seismic deployment enhances passive seismic monitoring for offshore CO_2 storage sites. By adding three broadband OBSs to the existing Norwegian National Seismic Network, we improved not only earthquake detection and location performance offshore, but also gained new constraints on shallow subsurface structure that di-

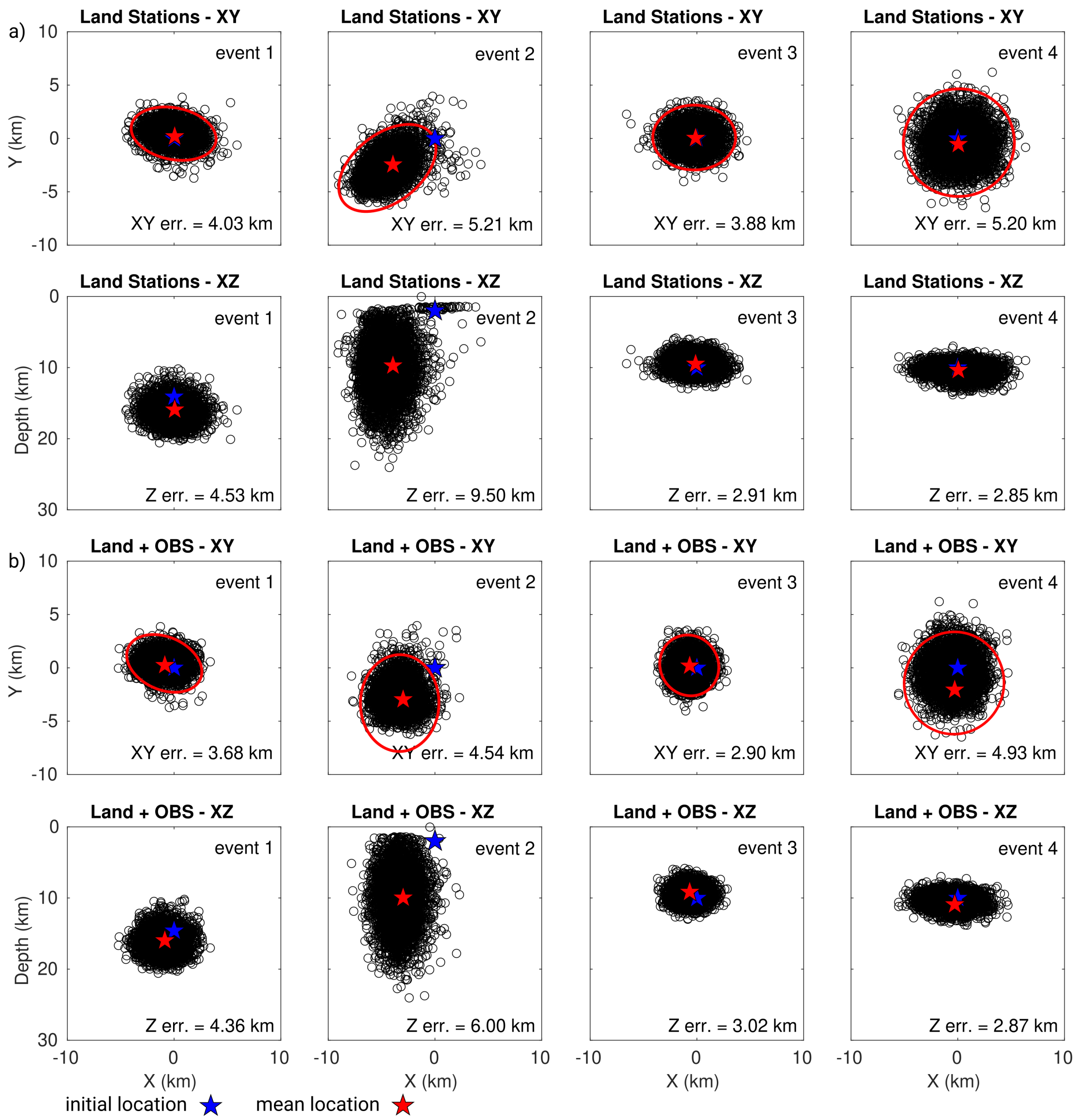

Figure 10 Example location distributions, in horizontal (X-Y planes) and vertical (X-Z planes) views for every 10th iteration for four example events located using land stations only (a) and a combination of OBS and land stations (b).

rectly influence seismic wave propagation and monitoring reliability.

The combination of machine-learning-based detection and the integration of OBS and land-based stations improves seismicity monitoring in the offshore Horda Platform region. The application of machine-learning-based detection increased the number of detected events and contributes to a reduction in the magnitude of completeness from Mc 1.1 to Mc 0.8, while the inclusion of OBS data enhances azimuthal coverage and reduces the geometric limitations of land-only monitoring. Although the increase in the number of detected events due to OBS data alone is modest, the improved network geometry provides better constraints on earthquake locations, particularly in offshore areas.

The expanded catalog reveals additional low-magnitude seismicity, mainly north of the Horda Platform, and provides a more robust baseline characterization of regional background seismicity in a stable intraplate setting. No seismicity was observed within the Aurora storage area during the monitoring period. This improved baseline is essential for distinguishing natural seismicity from potential future injection-related events associated with CO_2 storage.

Beyond detection improvements, the OBS data enabled direct observation of Scholte waves through ambient noise cross-correlation, providing valuable information on shallow offshore structure that cannot be obtained from land stations alone. The observed low group velocities (250-500 m/s) and surface wave modeling results indicate thick, low-velocity sedimentary sequences beneath the seafloor, requiring elevated V_P/V_S ratios of approximately 3.0. These shallow sedimentary layers strongly influence wave propagation, noise characteristics, and earthquake location accuracy, underscoring the importance of incorporating realistic near-surface structure into offshore velocity models.

Incorporating OBS recordings into Bayesian hierarchical relocation further improved confidence in earthquake locations by accounting for systematic travel-time differences between offshore and onshore paths. Although higher noise levels and complex near-surface conditions remain challenges for OBS-based monitoring, our results show that these limitations can be mitigated through modern detection algorithms, careful data processing, and appropriate velocity parameterization.

In summary, this study illustrates that targeted OBS deployments provide benefits that extend beyond improved detection thresholds. They provide additional structural information useful for interpreting offshore seismicity and to design reliable monitoring strategies for CO_2 storage projects. While permanent offshore monitoring with real-time telemetry remains the ideal solution, our results demonstrate that even short-term and thus more cost-effective OBS deployments may play a key role in establishing baseline seismicity, refining Earth models, and supporting containment and conformance assessments for offshore CO_2 storage initiatives such as the Aurora project.

Acknowledgements

We thank the Norwegian National Seismic Network, NORSAR, Equinor, British Geological Survey for providing seismological datasets used in this study. This work was carried out as part of the HNET Phase 3 project (https://hordanet.no/), funded as a CLIMIT Demo project with support from Gassnova, Equinor, Shell, TotalEnergies, CGG, and the Northern Lights Joint Venture DA. H.A.S also acknowledges the support of KAUST baseline BAS/1/1339-01-01 awarded to P.M.M. We thank the handling editor, Robert Skoumal, the anonymous reviewer and J. Ole Kaven for their constructive comments, which improved the manuscript.

Data and code availability

The earthquake catalog from the Norwegian National Seismic Network (NNSN) is available on the NNSN webpage (https://nnsn.geo.uib.no/nnsn). Continuous seismic data from the three OBSs deployed in this project, HNO1, HNO2, and HNO3 (network code: 7Y), the NNSN (network code: NS; University of Bergen, 1982), the NORSAR network (network code: NO; NORSAR, 1971; Schweitzer et al., 2021), and the HNAR Array (network code: QE; Equinor (Norway), 2020) are available through the UiB-NORSAR European Integrated Data Archive (EIDA) node (https://eida.geo.uib.no; Ottemöller et al., 2021). Data from the Great Britain Seismic Network (network code: GB; British Geological Survey, 1970) are available through the Data Management Center of NSF SAGE (https://ds.iris.edu/ds/nodes/dmc/). The Fault and oil field data are available on The Norwegian Offshore Directorate portal: https://factmaps.sodir.no/map/. The EGF measurement and timing verification were performed using EGF_td_toolbox (https://github.com/KarinaLov/EGF-time-correction-toolbox). The earthquake data processing were performed using EQtransformer package (https://eqtransformer.readthedocs.io), Obspy package (https://docs.obspy.org/) (Beyreuther et al., 2010; The ObsPy Development Team, 2020) and Seisan earthquake analysis software (http://seisan.info/). Figures in this article were generated using Matlab, Generic Mapping Tools (Wessel et al., 2013) and Inkscape, a vector graphics editor (https://inkscape.org/).

Competing interests

The authors have no competing interests.

References

Alsaker, A., Kvamme, L. B., Hansen, R. A., Dahle, A., and Bungum, H. The ML scale in Norway. *Bulletin of the Seismological Society of America*, 81(2):379–398, 1991. doi: 10.1785/BSSA0810020379.

Baird, A. F., Morten, J. P., Oye, V., and Bjørnstad, S. Ocean Space Surveillance and Real-Time Event Characterization Using Distributed Acoustic Sensing on Submarine Networks. *Seismological Research Letters*, 96(2A):691–705, 2025. doi: 10.1785/0220240360.

Bensen, G. D., Ritzwoller, M. H., Barmin, M. P., Levshin, A. L., Lin, F., Moschetti, M. P., Shapiro, N. M., and Yang, Y. Processing seismic ambient noise data to obtain reliable broad-band surface wave dispersion measurements. *Geophysical Journal International*, 169(3):1239–1260, 2007. doi: 10.1111/j.1365-246X.2007.03374.x.

Beyreuther, M., Barsch, R., Krischer, L., Megies, T., Behr, Y., and Wassermann, J. ObsPy: A Python Toolbox for Seismology. *Seismological Research Letters*, 81(3):530–533, 05 2010. doi: 10.1785/gssrl.81.3.530.

British Geological Survey. Great Britain Seismograph Network, 1970. doi: 10.7914/AV8J-NC83.

Bungum, H., Lindholm, C. D., and Dahle, A. Long-period ground-motions for large European earthquakes, 1905–1992, and comparisons with stochastic predictions. *Journal of Seismology*, 7(3):377–396, Jul 2003. doi: 10.1023/A:1024505229355.

Bussat, S. and Kugler, S. Offshore ambient-noise surface-wave tomography above 0.1 Hz and its applications. *The Leading Edge*, 30(5):514–524, 2011. doi: 10.1190/1.3589107.

Bussat, S., Bjerrum, L., Dando, B., Bergfjord, E., Iranpour, K., and Oye, V. Offshore injection and overburden surveillance using real-time passive seismic. *First Break*, 34(7), 2016. doi: 10.3997/1365-2397.34.7.86052.

Bussat, S., Houbiers, M., and Zarifi, Z. Real-time microseismic overburden surveillance at the Grane PRM field offshore Norway. *First Break*, 36(4):63–70, 2018. doi: 10.3997/1365-2397.n0084.

Chen, Y., Saad, O. M., Savvaidis, A., Chen, Y., and Fomel, S. 3D Microseismic Monitoring Using Machine Learning. *Journal of Geophysical Research: Solid Earth*, 127(3):e2021JB023842, 2022. doi: 10.1029/2021JB023842.

Corela, C., Loureiro, A., Duarte, J. L., Matias, L., Rebelo, T., and Bartolomeu, T. The effect of deep ocean currents on ocean-bottom seismometers records. *Natural Hazards and Earth System Sciences*, 23(4):1433–1451, 2023. doi: 10.5194/nhess-23-1433-2023.

Crowder, E., Rawlinson, N., Cornwell, D. G., Sammarco, C., Galetti, E., and Curtis, A. New insights into North Sea deep crustal structure and extension from transdimensional ambient noise tomography. *Geophysical Journal International*, 224(2): 1197–1210, 2021. doi: 10.1093/gji/ggaa475.

Cubas Armas, M., Ugalde, A., Monfret, T., Ventosa, S., Rodriguez, T., and Villaseñor, A. Integrating Submarine DAS into a Regional Seismic Network for Enhanced Offshore Earthquake Location: A Case Study from the Canary Islands. *Seismological Research Letters*, 2026. doi: 10.1785/0220250350.

Delaney, E., Ermert, L., Sager, K., Kritski, A., Bussat, S., and Fichtner, A. Passive seismic monitoring with nonstationary noise sources. *Geophysics*, 82(4):KS57–KS70, 2017. doi: 10.1190/geo2016-0330.1.

Demuth, A., Ottemöller, L., and Keers, H. Ambient noise levels and detection threshold in Norway. *Journal of Seismology*, 20(3): 889–904, 2016. doi: 10.1007/s10950-016-9566-8.

Dewangan, P., Reddy, R., Kamesh Raju, K. A., Singha, P., Aswini, K. K., Yatheesh, V., Samudrala, K., and Shuhail, M. Nature of the Ambient Noise, Site Response, and Orientation of Ocean-Bottom Seismometers (OBSs): Scientific Results of a Passive Seismic Experiment in the Andaman Sea. *Bulletin of the Seismological Society of America*, 108(1):248–259, 2017. doi: 10.1785/0120170163.

Doran, A. K. and Laske, G. Ocean-Bottom Seismometer Instrument Orientations via Automated Rayleigh-Wave Arrival-Angle Measurements. *Bulletin of the Seismological Society of America*, 107 (2):691–708, 2017. doi: 10.1785/0120160165.

Eigestad, G. T., Dahle, H. K., Hellevang, B., Riis, F., Johansen, W. T., and Øian, E. Geological modeling and simulation of CO_2 injection in the Johansen formation. *Computational Geosciences*, 13 (4):435–450, 2009. doi: 10.1007/s10596-009-9134-3.

Ellsworth, W. L. Injection-Induced Earthquakes. *Science*, 341 (6142):1225942, 2013. doi: 10.1126/science.1225942.

Equinor (Norway). Equinor network is designed for passive monitoring of the CO2 storage sites in offshore Norway, 2020. doi: 10.7914/SN/QE.

Fazlikhani, H., Fossen, H., Gawthorpe, R. L., Faleide, J. I., and Bell, R. E. Basement structure and its influence on the structural configuration of the northern North Sea rift. *Tectonics*, 36(6): 1151–1177, 2017. doi: 10.1002/2017TC004514.

Fejerskov, M. and Lindholm, C. Crustal stress in and around Norway: an evaluation of stress-generating mechanisms. *Geological Society, London, Special Publications*, 167(1):451–467, 2000. doi: 10.1144/GSL.SP.2000.167.01.19.

Frazão, Orlando, Silva, Susana, Corela, Carlos, Loureiro, Afonso, Gonçalves, Susana, Robalinho, Paulo, Sousa, Ricardo, Martins, Hugo F., Carrilho, Fernando, Omira, Rachid, Niehus, Manfred, and Matias, Luis. Comparison of seismic records obtained by distributed acoustic sensing and ocean bottom seismometers. *J. Eur. Opt. Society-Rapid Publ.*, 22(1):11, 2026. doi: 10.1051/jeos/2026007.

Funck, T., Geissler, W. H., Kimbell, G. S., Gradmann, S., Ögmundur Erlendsson, McDermott, K., and Petersen, U. K. Moho and basement depth in the NE Atlantic Ocean based on seismic refraction data and receiver functions. *Geological Society, London, Special Publications*, 447(1):207–231, 2017. doi: 10.1144/SP447.1.

Furre, A.-K., Meneguolo, R., Ringrose, P., and Kassold, S. Building confidence in CCS: From Sleipner to the Northern Lights Project. *First Break*, 37(7):81–87, 2019. doi: 10.3997/1365-2397.n0038.

Ge, S. and Saar, M. O. Review: Induced Seismicity During Geoenergy Development—A Hydromechanical Perspective. *Journal of Geophysical Research: Solid Earth*, 127(3):e2021JB023141, 2022. doi: 10.1029/2021JB023141.

Goertz-Allmann, B. P., Kühn, D., Oye, V., Bohloli, B., and Aker, E. Combining microseismic and geomechanical observations to interpret storage integrity at the In Salah CCS site. *Geophysical Journal International*, 198(1):447–461, 2014. doi: 10.1093/gji/ggu010.

Grigoli, F., Cesca, S., Rinaldi, A. P., Manconi, A., López-Comino, J. A., Clinton, J. F., Westaway, R., Cauzzi, C., Dahm, T., and Wiemer, S. The November 2017 <i>M</i>_w 5.5 Pohang earthquake: A possible case of induced seismicity in South Korea. *Science*, 360(6392):1003–1006, 2018. doi: 10.1126/science.aat2010.

Hable, S., Sigloch, K., Barruol, G., Stähler, S. C., and Hadzi-ioannou, C. Clock errors in land and ocean bottom seismograms: high-accuracy estimates from multiple-component noise cross-correlations. *Geophysical Journal International*, 214 (3):2014–2034, 2018. doi: 10.1093/gji/ggy236.

Havskov, J. and Bungum, H. Source parameters for earthquakes in the northern North Sea. *Norsk Geologisk Tidsskrift*, (67):51–58, 1987.

Havskov, J. and Ottemoller, L. SeisAn Earthquake Analysis Software. *Seismological Research Letters*, 70(5):532–534, 1999. doi: 10.1785/gssrl.70.5.532.

Havskov, J. and Ottemöller, L. *Routine Data Processing in Earthquake Seismology: With Sample Data, Exercises and Software*. Springer, 2010. doi: 10.1007/978-90-481-8697-6.

Havskov, J., Voss, P. H., and Ottemöller, L. Seismological Observatory Software: 30 Yr of SEISAN. *Seismological Research Letters*, 91(3):1846–1852, 2020. doi: 10.1785/0220190313.

Herrmann, R. B. Computer Programs in Seismology: An Evolving Tool for Instruction and Research. *Seismological Research Letters*, 84(6):1081–1088, 11 2013. doi: 10.1785/0220110096.

Holden, N., Osmond, J. L., Mulrooney, M. J., Braathen, A., Skurtveit, E., and Sundal, A. Structural characterization and across-fault seal assessment of the Aurora CO₂ storage site, northern North Sea. *Petroleum Geoscience*, 28(4): petgeo2022–036, 2022. doi: 10.1144/petgeo2022-036.

Jeddi, Z., Ottemöller, L., Sørensen, M. B., Rezaei, S., Gibbons, S. J., Strømme, M. L., Voss, P. H., and Dahl-Jensen, T. Improved Seismic Monitoring with OBS Deployment in the Arctic: A Pilot Study from Offshore Western Svalbard. *Seismological Research Letters*, 92(5):2705–2717, 2021. doi: 10.1785/0220200471.

Jerkins, A. E., Shiddiqi, H. A., Kværna, T., Gibbons, S. J., Schweitzer, J., Ottemöller, L., and Bungum, H. The 30 June 2017 North Sea Earthquake: Location, Characteristics, and Context. *Bulletin of the Seismological Society of America*, 110(2):937–952, 2020. doi: 10.1785/0120190181.

Jerkins, A. E., Oye, V., Alvizuri, C., Halpaap, F., and Kværna, T. The 21 March 2022 Mw 5.1 Tampen Spur Earthquake, North Sea: Location, Moment Tensor, and Context. *Bulletin of the Seismological Society of America*, 114(2):741–757, 2023. doi: 10.1785/0120230163.

Kaven, J. O., Hickman, S. H., McGarr, A. F., and Ellsworth, W. L. Surface Monitoring of Microseismicity at the Decatur, Illinois, CO2 Sequestration Demonstration Site. *Seismological Research Letters*, 86(4):1096–1101, 06 2015. doi: 10.1785/0220150062.

Kugler, S., Bohlen, T., Forbriger, T., Bussat, S., and Klein, G. Scholte-wave tomography for shallow-water marine sediments. *Geophysical Journal International*, 168(2):551–570, 2007. doi: 10.1111/j.1365-246X.2006.03233.x.

Landrø, M., Bouffaut, L., Kriesell, H. J., Potter, J. R., Rørstadbotnen, R. A., Taweesintananon, K., Johansen, S. E., Brenne, J. K., Haukanes, A., Schjelderup, O., and Storvik, F. Sensing whales, storms, ships and earthquakes using an Arctic fibre optic cable. *Scientific Reports*, 12(1):19226, 2022. doi: 10.1038/s41598-022-

23606-x.

Lee, A. W. THE NORTH SEA EARTHQUAKE OF 1927 JANUARY 24. *Geophysical Journal International*, 3(s1):21–30, 1932. doi: 10.1111/j.1365-246X.1932.tb03655.x.

Lienert, B. R. and Havskov, J. A computer Program for Locating Earthquakes Both Locally and Globally. *Seismological Research Letters*, 66(5):26–36, 1995. doi: 10.1785/gssrl.66.5.26.

Loviknes, K. *Measuring seismic station timing errors from ambient noise*. Master thesis, University of Bergen, 2018. https://bora.uib.no/bora-xmlui/handle/1956/18942.

Loviknes, K., Jeddi, Z., Ottemöller, L., and Barreyre, T. When Clocks Are Not Working: OBS Time Correction. *Seismological Research Letters*, 91(4):2247–2258, 2020. doi: 10.1785/0220190342.

Marck, A., Ottemöller, L., Rondenay, S., and Fossen, H. Intraplate seismicity in southwestern Norway: enhanced catalogue highlights diffusive earthquake occurrence linked to inherited weakness zones. *Geophysical Journal International*, 240 (3):2006–2022, 2025. doi: 10.1093/gji/ggaf018.

McNamara, D. E. and Buland, R. P. Ambient Noise Levels in the Continental United States. *Bulletin of the Seismological Society of America*, 94(4):1517–1527, 2004. doi: 10.1785/012003001.

Mousavi, S. M., Sheng, Y., Zhu, W., and Beroza, G. C. STanford EArthquake Dataset (STEAD): A Global Data Set of Seismic Signals for AI. *IEEE Access*, 7:179464–179476, 2019. doi: 10.1109/ACCESS.2019.2947848.

Mousavi, S. M., Ellsworth, W., Weiqiang, Z., Chuang, L., and Beroza, G. Earthquake transformer—an attentive deep-learning model for simultaneous earthquake detection and phase picking. *Nature Communications*, 11:3952, 08 2020. doi: 10.1038/s41467-020-17591-w.

Myers, S. C., Johannesson, G., and Hanley, W. A Bayesian hierarchical method for multiple-event seismic location. *Geophysical Journal International*, 171(3):1049–1063, 2007. doi: 10.1111/j.1365-246X.2007.03555.x.

Myers, S. C., Johannesson, G., and Hanley, W. Incorporation of probabilistic seismic phase labels into a Bayesian multiple-event seismic locator. *Geophysical Journal International*, 177(1): 193–204, 2009. doi: 10.1111/j.1365-246X.2008.04070.x.

Naranjo, D., Parisi, L., Jónsson, S., Jousset, P., Werthmüller, D., and Weemstra, C. Ocean bottom seismometer clock correction using ambient seismic noise. *Seismica*, 3(1), 2024. doi: 10.26443/seismica.v3i1.367.

Nguyen, X. N., Dahm, T., and Grevemeyer, I. Inversion of Scholte wave dispersion and waveform modeling for shallow structure of the Ninetyeast Ridge. *Journal of Seismology*, 13(4):543–559, Oct 2009. doi: 10.1007/s10950-008-9145-8.

NORSAR. NORSAR Station Network [Data set], 1971. doi: 10.21348/d.no.0001.

Ottemöller, L., Strømme, M. L., and Storheim, B. M. *Seismic monitoring and data processing at the Norwegian National Seismic Network*, volume 52, chapter Summary of the Bulletin of the International Seismological Centre 2015 January-June, pages 27–40. International Seismological Centre, Thatcham, United Kingdom, 2018. doi: 10.31905/1M97CSYL.

Ottemöller, L., Michalek, J., Christensen, J.-M., Baadshaug, U., Halpaap, F., Natvik, o., Kværna, T., and Oye, V. UiB-NORSAR EIDA Node: Integration of Seismological Data in Norway. *Seismological Research Letters*, 2021. doi: 10.1785/0220200369.

Parisi, L., Augustin, N., Trippanera, D., Kirk, H., Dannowski, A., Matrau, R., Fittipaldi, M., Nobile, A., Zielke, O., Valero Cano, E., Hoogewerf, G., Aspiotis, T., Manzo-Vega, S., Espindola Carmona, A., Barreto, A., Juchem, M., Suhendi, C., Schmidt-Aursch, M., Mai, P. M., and Jónsson, S. The First Network of Ocean Bottom Seismometers in the Red Sea to Investigate the Zabargad Fracture Zone. *Seismica*, 3(1), Apr. 2024. doi: 10.26443/seismica.v3i1.729.

Peterson, J. R. Observation and Modeling of Seismic Background Noise. Open-File Report 93-322, U.S. Geological Survey, 1993. doi: 10.3133/ofr93322.

Pilot, M., Lien, M. J., Schlindwein, V., Ottemöller, L., and Barreyre, T. Microseismicity Around Loki's Castle Hydrothermal Vent Field Reveals the Early Stages of Detachment Faulting at the Mohns-Knipovich Ridge Intersection. *Geochemistry, Geophysics, Geosystems*, 25(12):e2024GC011732, 2024. doi: 10.1029/2024GC011732.

Rathnayaka, S. and Gao, H. Crustal-Scale Seismic Structure From Trench to Forearc in the Cascadia Subduction Zone. *Journal of Geophysical Research: Solid Earth*, 122(9):7311–7328, 2017. doi: 10.1002/2017JB014299.

Ringdal, F. Seismicity of the North Sea Area. In Ritsema, A. R. and Gürpinar, A., editors, *Seismicity and Seismic Risk in the Offshore North Sea Area*, pages 53–75. Springer Netherlands, Dordrecht, 1983.

Schultz, R., Baptie, B., Edwards, B., and Wiemer, S. Red-light thresholds for induced seismicity in the UK. *Seismica*, 2(2), Oct. 2023. doi: 10.26443/seismica.v2i2.1086.

Schweitzer, J., Köhler, A., and Christensen, J. M. Development of the NORSAR Network over the Last 50 Yr. *Seismological Research Letters*, 92(3):1501–1511, 2021. doi: 10.1785/0220200375.

Shen, S., Zheng, J., Sun, Y., Teng, X., and Peng, S. A Continuous Data Acquisition System for Three-Component Surface Microseismic Real-Time Monitoring. *IEEE Sensors Journal*, 22(21): 20635–20644, 2022. doi: 10.1109/JSEN.2022.3208442.

Shiddiqi, H. A., Ottemöller, L., Rondenay, S., Custódio, S., Gahalaut, V. K., Yadav, R. K., Halpaap, F., and Gahalaut, K. Seismicity modulation due to hydrological loading in a stable continental region: a case study from the Jektvik swarm sequence in Northern Norway. *Geophysical Journal International*, 235(1):231–246, 2023a. doi: 10.1093/gji/ggad210.

Shiddiqi, H. A., Ottemöller, L., Rondenay, S., Custódio, S., Halpaap, F., and Gahalaut, V. K. Comparison of Earthquake Clusters in a Stable Continental Region: A Case Study from Nordland, Northern Norway. *Seismological Research Letters*, 94(3):1627–1642, 2023b. doi: 10.1785/0220220325.

Shiddiqi, H. A., Parisi, L., Valero Cano, E., Fittipaldi, M., Augustin, N., Baby, G., Mai, P. M., and Jónsson, S. Transform Faulting in the Northern Red Sea Revealed by Ocean Bottom Seismometers Deployed in the Zabargad Fracture Zone. *Geochemistry, Geophysics, Geosystems*, 26(8):e2025GC012253, 2025. doi: 10.1029/2025GC012253.

The ObsPy Development Team. ObsPy 1.2.2, 2020. doi: 10.5281/zenodo.3921997.

Thompson, N., Andrews, J. S., Wu, L., and Meneguolo, R. Characterization of the in-situ stress on the Horda platform – A study from the Northern Lights Eos well. *International Journal of Greenhouse Gas Control*, 114:103580, 2022. doi: 10.1016/j.ijggc.2022.103580.

University of Bergen. University of Bergen Seismic Network, 1982. doi: 10.7914/SN/NS.

Verliac, M. and Calvez, J. L. Microseismic monitoring for reliable CO2 injection and storage — Geophysical modeling challenges and opportunities. *The Leading Edge*, 40(6):418–423, 2021. doi: 10.1190/tle40060418.1.

Wessel, P., Smith, W. H. F., Scharroo, R., Luis, J., and Wobbe, F. Generic Mapping Tools: Improved Version Released. *Eos, Transactions American Geophysical Union*, 94(45):409–410, 2013. doi:

10.1002/2013EO450001.

Wiemer, S. and Wyss, M. Minimum Magnitude of Completeness in Earthquake Catalogs: Examples from Alaska, the Western United States, and Japan. *Bulletin of the Seismological Society of America*, 90(4):859–869, 2000. doi: 10.1785/0119990114.

Zarifi, Z., Köhler, A., Ringrose, P., Ottemöller, L., Furre, A., Hansteen, F., Jerkins, A., Oye, V., Dehghan Niri, R., and Bakke, R. Background Seismicity Monitoring to Prepare for Large-Scale CO2 Storage Offshore Norway. *Seismological Research Letters*, 94(2A):775–791, 2022. doi: 10.1785/0220220178.

Zoback, M. D. and Gorelick, S. M. Earthquake triggering and large-scale geologic storage of carbon dioxide. *Proceedings of the National Academy of Sciences*, 109(26):10164–10168, 2012. doi: 10.1073/pnas.1202473109.